

# Enhancing Indoor Localization Accuracy Using a Hybrid Deep Learning Algorithm: A DNN-CNN Approach

Hossein Asadollahi<sup>✉</sup>, Nader Mokari<sup>✉</sup>, Senior Member, IEEE,  
Hamid Saeedi<sup>✉</sup>, Member, IEEE, Halim Yanikomeroglu<sup>✉</sup>, Fellow, IEEE

**Abstract**—Indoor localization within buildings is paramount due to its diverse applications, including the Internet of Things (IoT), healthcare, and personnel monitoring. To improve the performance of indoor localization, this study proposes an algorithm combining Deep Neural Networks (DNNs) and Convolutional Neural Networks (CNNs) used within a hybrid model that uses both cellular technology, i.e., base station (BS) and Wi-Fi access point (AP). Within a realistic environment, we evaluate the performance of our approach across four scenarios: (1) (2 APs + 2 BSs), (2) (1 AP + 2 BSs), (3) (2 APs), and (4) (2 BSs). Additionally, we consider both stationary and seated user positions. Our results demonstrate significant improvements over existing methods. Specifically, in the 2 APs+2 BSs scenario, we achieve an average Euclidean distance error of 1.04 meters, with a maximum error of 2.51 meters, and the Root Mean Square Error (RMSE) of 1.15 meters. We also obtain the corresponding Cumulative Distribution Function (CDF) for the error which indicates that 90% of the time, the error is less than 1.69 meters. Our hybrid model achieves over 99% accuracy in classifying different building floors and over 88% accuracy in identifying user states (e.g., standing or sitting). We validate our approach using smartphone-based indoor localization in a two-story residential building with robust construction materials and double-layered walls.

**Index Terms**—Localization, artificial intelligence, fingerprint-based positioning, cellular, Wi-Fi

## I. INTRODUCTION

WITH the proliferation of communication technologies and the Internet of Things, the importance and application of indoor localization for user equipment are increasing day by day. Some applications of indoor localization include elderly and patient care, personnel control in a company, inventory management, estimation of building occupancy, control of heating and cooling equipment in a building, smart advertising, and many other diverse applications [1]–[3].

Various indoor localization technologies include Bluetooth, Wi-Fi, ultra-wideband (UWB), cellular, and others. Bluetooth technology has low energy consumption but limited range, low localization accuracy, and interference with other waves.

Hossein Asadollahi is with the Faculty of Electrical and Computer Engineering, Tarbiat Modares University, Tehran 1411713116, Iran (e-mail: h.asadollahi@modares.ac.ir); Nader Mokari is with the Faculty of Electrical and Computer Engineering, Tarbiat Modares University, Tehran 1411713116, Iran (e-mail: mokari@modares.ac.ir); Hamid Saeedi is with the College of Engineering and Technology, University of Doha for Science and Technology, Doha, Qatar (e-mail: hamid.saeedi@udst.edu.qa); Halim Yanikomeroglu is with the Department of Systems and Computer Engineering, Carleton University, Ottawa, ON K1S 5B6, Canada (e-mail: halim@sce.carleton.ca);

Additionally, deployment entails high equipment costs [4], [5]. In contrast, Wi-Fi offers a broader coverage range, greater penetration power through buildings and walls, and higher localization accuracy than Bluetooth, albeit with higher energy consumption. However, signal interference is possible, especially when devices are in close proximity. This technology requires more equipment for precise user localization, thus increasing costs [6]–[11]. UWB utilizes signals with high bandwidth, penetration power, and high accuracy. It is unaffected by multi-path effects and walls but is primarily used for short-range communications and requires additional equipment. Limited research has been conducted on this technology, and it is not common in current user devices [12], [13].

Among the said technologies, cellular technology is also shown to be very effective in localization. It requires no special equipment, its coverage range is vast and it has greater penetration power compared to other technologies. Location-based services have become standard in different cellular network generations, with increasing accuracy with each generation's advancement. Moreover, with higher generations and frequencies, signal penetration into buildings increases. This technology significantly reduces user-side costs and has no signal interference [2], [14]–[21]. However, the accuracy of cellular technology is not as high as that of Wi-Fi and other technologies. Hence, in this article, we combine cellular technology with Wi-Fi to enhance accuracy [5], [15], [16], [21]–[24]. Indeed, Wi-Fi serves as a complementary tool in this study, with the main focus on cellular technology.

In the field of indoor localization, various techniques exist, including Angle of Arrival (AoA), Time Difference of Arrival (TDoA), and fingerprinting. TDoA and AoA require precise synchronization between transmitter and receiver, where increased synchronization accuracy enhances localization accuracy. These techniques necessitate additional and specialized equipment [25], [26]. However, the fingerprinting technique relies on map-based location and consists of offline and online components. In the offline phase, the environment map is obtained, signal measurements are taken at reference points, and the results are stored in a database with location tags. Upon completing the database, in the online phase, user location is determined through parameter measurement and database matching [7], [10], [14], [27]–[31]. Received Signal Strength Indicator (RSSI) and Channel State Information (CSI) signal parameters are utilized in the fingerprinting technique. While the CSI parameters are complex and require equipment

and algorithms for feature extraction [32]–[34], RSSI can be easily measured and recorded using smartphones [2], [20], [28], [31]. Hence, in this article, RSSI signal values from various reference points are measured using a smartphone to create a fingerprint database. Subsequently, the database is trained with a designed neural network, and in the online phase, the neural network is used to estimate user position.

In this paper, we significantly improve the performance and efficiency of indoor localization by combining various neural networks and data preparation methods. This research is conducted in a realistic environment using a smartphone, urban Base Stations (BSs) signals, and indoor Access Points (APs). This study aims at enhancing indoor localization based on BS signals, achieved through two main strategies: 1) Utilizing a minimal number of indoor APs as auxiliary technology, and 2) designing an Artificial Intelligence (AI) model capable of accurately estimating the user's location even in the worst-case scenarios. The scenarios used in this research account for various user conditions and environmental signal status. The primary innovation of this paper lies in the hybrid AI model. Additionally, we use innovative methods in scenario design, testing environment, and data preparation. The study results indicate that our model outperforms many traditional algorithms in indoor localization.

The rest of this article is organized as follows: Section II reviews the related works pertinent to our study, providing an overview of the existing literature and methodologies and highlighting the gaps that this study seeks to address. In Section III, we delve into the implemented model, offering a detailed description of its architecture. Section IV outlines the governing equations central to our problem, presenting the theoretical foundation and mathematical formulation employed. Section V presents the experimental results, showcasing the performance and validation of our model through various tests and benchmarks. Finally, Section VI concludes the paper with a discussion of the findings, their implications, and potential directions for future research.

## II. RELATED WORK

In the field of indoor localization, researchers have undertaken numerous studies and continually strive to enhance user location accuracy through innovative techniques and various technologies [3], [4], [6], [17], [31], [34]–[42]. However, the application of fingerprinting techniques and RSSI parameters with cellular technology has received less attention.

Lembo and colleagues conducted a study comparing the performance of Neural Networks (NN) and Genetic Algorithms (GA) in indoor localization. This research involved two-dimensional localization of user equipment across three separate floors, utilizing eight indoor Pico BSs. The employed technique was fingerprinting with the RSSI parameter. RSSI values were recorded using a mobile robot equipped with devices such as two Qualcomm Long-Term Evolution (LTE) modems, LIDAR and Keysight Nemo. Due to the variation in Cumulative Distribution Function (CDF) values across floors, the 75th CDF percentile level error exceeded 4 meters on two floors and 2.5 meters on one floor. Additionally, for 50th CDF percentile, the GA algorithm outperforms the NN [31].

Another study by Chai and colleagues explored two scenarios. In the first scenario, the RSSI of six types of cellular network signals was combined with the signals from 30 APs, and the user's location was estimated using the Manhattan-KNN (K-Nearest Neighbors) algorithm with  $K = 4$ . This scenario reported an average error of 1.6 meters, a maximum error of 5.51 meters, a Root Mean Square Error (RMSE) of 1.96, where error was less than 4 meters 90% of the times. In the second scenario, the cellular network was used to determine an area, and APs were used to pinpoint the user's exact location. This scenario exhibited worse localization errors than the first, with an average user location error of 3.91 meters, a maximum error of 39.24 meters, and an RMSE of 1.96. The cellular network signals used in this study included FD-LTE, WCDMA, CDMA, TD-LTE, TD-SCDMA, and GSM. RSSI measurements were taken using a smartphone and a specific application [24].

Lee and colleagues researched indoor localization using the fingerprint technique in cellular networks. For each Physical Cell ID (PCI), an RSSI matrix was formed and augmented with Gaussian regression to create the fingerprint database. For test data, an RSSI matrix was generated, and correlation at each test point was calculated with the database matrix based on Euclidean distance. This research was conducted using a smartphone in an underground shopping mall connected to a metro station. Measurements were taken in three scenarios, yielding RMSE values of 2.82, 2.64, and 2.3 meters, respectively, and 90th CDF percentile values of 4.6, 4.8, and 5.1 meters, respectively [19].

Lastly, the research by Zheng and colleagues aimed to enhance localization accuracy using the WKNN algorithm. This study improved localization precision by 13.58% through techniques such as classifying test areas, removing outlier data, and applying a Kalman filter. These methods reduced the localization error from 3.64 meters to 2.77 meters. RSSI measurements were conducted using a smartphone and specialized software. The testing environment included nine small indoor BSs, forming a dedicated LTE network [17].

In several previous studies, numerous different devices and signals are used in cellular networks and APs. Additionally, these devices are often customized and not fully aligned with the configurations of real-world operators, leading to high costs for the localization system and insufficient accuracy based on actual data. While these studies contribute significantly to the development of science, the algorithms used are either traditional or fail to provide the accuracy required for indoor localization. Moreover, these algorithms are only examined in a single domain, failing to meet other needs of the localization system.

In our research, we utilize a minimal number of signals and equipment both inside and outside the building. We use one AP per floor for indoor equipment, and we consider two urban BS for outdoor equipment. Each BS is studied with only one PCI. Furthermore, the designed neural network model meets the needs of indoor localization, including floor detection, location determination, and user state identification on each floor. This model is capable of making accurate estimations under various signal conditions.

### III. IMPLEMENTED MODEL REVIEW

This section begins with analyzing the RSSI parameter, emphasizing its role and importance in wireless communication and indoor localization. Following this, we provide an overview of the software and hardware used in our system, including the specifications and configurations of the devices and platforms employed. Finally, we introduce our designed neural network model, describing its architecture, training process, and innovative techniques to enhance its efficacy.

#### A. Received Signal Strength Indicator (RSSI)

RSSI is a critical parameter in wireless communication that measures the power level of a received signal. It is a fundamental metric for various applications, including indoor localization, network management, and signal quality assessment. RSSI values provide insight into a device's proximity to a transmitter and the quality of the received signal, which is essential for optimizing wireless networks and improving location-based services [43].

RSSI is usually measured in decibels per milliwatt (dBm) and is a logarithmic measure of the power in a received radio signal. Calculation of RSSI involves several key factors, including transmit power, distance between transmitter and receiver, and environmental conditions that may cause signal attenuation or interference. (1) shows how to calculate this parameter [35], [40], [44]:

$$RSSI = 10 \log_{10} \left( \frac{P_{\text{received}}}{P_{\text{reference}}} \right), \quad (1)$$

where  $P_{\text{received}}$  represents the power of the received signal in milliwatts, and  $P_{\text{reference}}$  represents the reference power, which is one milli watt. One of the most common models used to estimate RSSI is the path loss model, which describes how signal strength decreases with distance as in (2) [2], [20], [45]–[47]:

$$RSSI(d) = RSSI(d_0) - 10n \log_{10} \left( \frac{d}{d_0} \right), \quad (2)$$

where  $RSSI(d)$  indicates the strength of the received signal at the distance  $d$  and  $RSSI(d_0)$  is the strength of the received signal at the reference distance  $d_0$ .  $n$  is the path loss exponent, which varies depending on the environment (typically between 2 and 4 for indoor environments).

#### B. Software and Hardware Used in the Experiment

The equipment used in this study is categorized into software and hardware components. For the software category, three programs are utilized for measuring, recording, and processing data. These software tools are:

1. cellular-z: Used for recording and capturing RSSI values and other characteristics of cellular network signals [41].
2. RSSI\_Logger: Deployed for measuring and recording RSSI values of Wi-Fi networks [48].
3. MATLAB: Utilized for data processing and executing localization and AI algorithms.

Fig. 1 displays examples of data from cellular-z and RSSI\_Logger software.

Five pieces of equipment are used in the hardware category, including a Xiaomi Poco X3 Pro smartphone with a plastic and wooden stand, two D-Link routers to enhance indoor localization accuracy, and an Acer NIRO 5 laptop for processing tasks. The laptop used in the experiment, consists of a Core i7-11800H processor, 16GB DDR4 RAM, 1TB SSD, and an NVIDIA RTX 3050 4GB graphics card. Fig. 2 shows the hardware equipment.

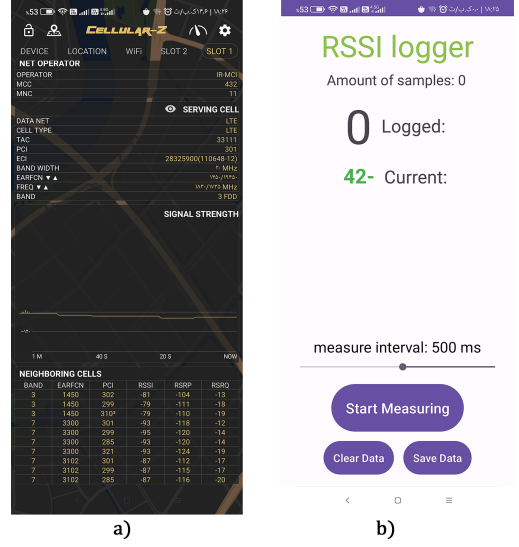


Fig. 1. A view of the used software: a) cellular-z software b) RSSI\_Logger software.



Fig. 2. A view of the hardware used: a) D-Link equipment b) Mobile phone holder base.

#### C. Examining the Designed Neural Network Model

The measured data from BS and AP in this experiment exhibit significant regression issues. Therefore, it is essential to use AI models that can extract deep features and details from the data and effectively learn the complex and difficult relationships between them to address the regression problem. There are various neural network models that can achieve this, such as CNN, DNN, LSTM (Long Short-Term Memory), etc [2], [9], [10], [22], [23], [27]–[29], [36], [38], [41], [42], [49]–[52]. In this study, we implement a hybrid DNN-CNN model with the network configurations described below. The selection of this model is entirely empirical. We also implement other neural networks such as CNN, DNN, LSTM, and AI algorithms such as KNN, SVM (support vector machine), and decision trees with the same settings

to show the superiority and efficiency of our work compared to other algorithms and neural networks. Our hybrid model features between six to twelve input neurons and one to two output neurons, depending on the scenario. For two-dimensional location estimation, it uses two output neurons, and for estimating floors and user states, it employs one output neuron. Following the input layer, the network transitions to the DNN, which consists of four layers, each containing 950 neurons with a tangent hyperbolic activation function. The patterns and features obtained from the DNN are then fed into a one-dimensional CNN layer (1D-CNN), which has 40 filters with a size of 30. The CNN layer not only extracts deep features but also reduces the dimensions of the data, enhancing processing efficiency. Finally, the data passes through a fully connected (FC) layer and a regression layer. Fig. 3 illustrates the designed neural network model. This network has established an excellent superiority over other networks in the field of indoor positioning based on cellular network with fingerprint technique and RSSI parameter. The CNN and

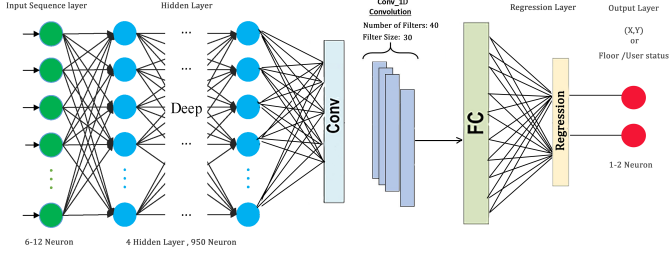


Fig. 3. A view of the designed neural network.

DNN, which we examine separately for comparison with the hybrid model, consist of the same components as the designed network. Specifically, the CNN, corresponds to the latter part of the hybrid model, while the DNN represents the initial part of the hybrid model. This comparison demonstrates how the combination of these two AI models significantly enhances the accuracy and performance of localization. Additionally, the LSTM network features a single layer with 300 hidden units, and the KNN algorithm was examined with  $K = 3$ . Fig. 4 illustrates the structure of the LSTM and KNN networks. For a deeper understanding of these network structures, one can refer to the works [53], [54].

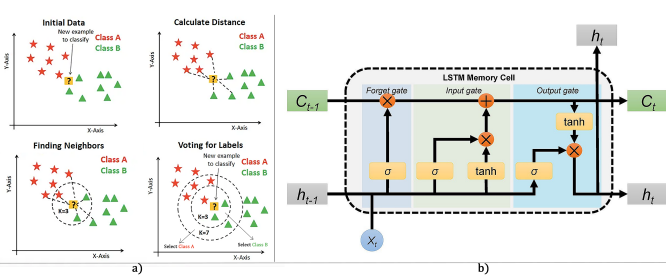


Fig. 4. A view of the structure of some AI models: a) view of KNN, b) view of LSTM unit.

#### D. Analysis of Indoor Localization Scenarios

This part describes and explains the scenarios implemented in this experiment. We assume four different conditions to test the performance, efficiency, and stability of our neural network. Initially, we hypothesize that the test environment includes two APs and one BS from the operator *MCI* (Mobile Communication Company of Iran) and another BS from the operator *MTN-Irancell*. In this case, APs can assist in locations where BS signals are weak. In the second scenario, we remove one AP to evaluate the system's behavior under conditions of failure and deficiency. In the third scenario, we eliminate the BSs and assess the conditions using only two APs. Finally, we keep only the BSs and conduct localization using cellular network signals. The cellular technology used in these experiments is LTE. Fig. 5 illustrates the test scenarios.

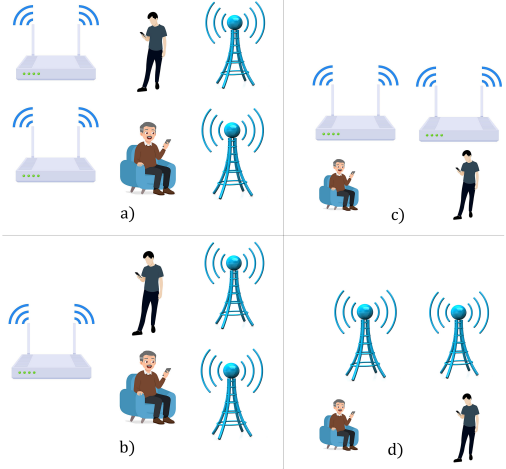


Fig. 5. Tested scenarios.

#### E. Measurement Criteria for Indoor Localization

In this section, we examine the metrics used to evaluate the accuracy of localization. This study employs three metrics: Distance Error (DE), RMSE, and CDF. The Distance Error is calculated based on the Euclidean distance [32], [55]–[57]. The RMSE used in this research includes both one-dimensional and two-dimensional RMSE.

For each point  $i$ , the DE is calculated as

$$DE_i = \sqrt{(\hat{x}_i - x_i)^2 + (\hat{y}_i - y_i)^2}, \quad (3)$$

where  $(x, y)$  is the actual location coordinates,  $(\hat{x}, \hat{y})$  is the estimated location coordinates.

One-dimensional RMSE's with respect to  $x$  and  $y$  coordinates are calculated as

$$RMSE_x = \sqrt{\frac{1}{N} \sum_{i=1}^N (\hat{x}_i - x_i)^2}, \quad (4)$$

$$RMSE_y = \sqrt{\frac{1}{N} \sum_{i=1}^N (\hat{y}_i - y_i)^2}. \quad (5)$$

For two-dimensional RMSE we have:

$$\begin{aligned} \text{RMSE2D} &= \sqrt{\frac{1}{N} \sum_{i=1}^N [(\hat{x}_i - x_i)^2 + (\hat{y}_i - y_i)^2]} \\ &= \sqrt{\text{RMSE}_x + \text{RMSE}_y}. \end{aligned} \quad (6)$$

Finally we have the CDF which is defined as below for a random variable  $X$ :

$$F_X(x) = \mathbf{P}(X \leq x). \quad (7)$$

#### IV. GOVERNING EQUATIONS OF THE PROBLEM

Our research is an experimental study using artificial intelligence models. Consequently, the mathematical relationships governing it constrain to the mathematical relationships of the neural network layers and the pre-processing applied to the data. Due to the small scale and proximity of location data points to each other, the neural network fails to learn the data thoroughly and cannot differentiate between some of them. To address this issue, we add a fixed number to the location data  $(x, y)$ .

The designed network consists of various components, including the input data layer, DNN and the functions used in it, CNN, and finally, an FC layer. The input layer, also known as the sequence input layer, inputs data sequences into the neural network and can perform various operations, such as normalization, depending on the network settings. However, in this study, the input layer does not perform any specific operations. The DNN is essentially a Multi-Layer Perceptron (MLP), typically with at least 3 hidden layers [58]. The functioning of the DNN is such that each neuron in the next layer receives information from all the neurons in the previous layer. Specifically, each neuron calculates the sum of the products of the weights and the features of the previous neurons and then adds a bias term. Finally, this value is passed through an activation function, which is tangent hyperbolic in this research, before being transferred to the next layer [59]–[61]:

$$\tanh(b_m + \sum_{i=1}^n P_i w_i). \quad (8)$$

In (8),  $m$  denotes the target neuron number,  $n$  is the maximum number of input to neurons,  $w_i$ 's are the input weights to neuron  $m$ ,  $P_i$ 's are the corresponding features, and  $b$  is the bias associated to neuron  $m$ . The performance of DNN can be seen in (8) and Fig. 6.

Next, we proceed to a 1D-CNN, where the features and information from the last layer of the DNN are fed into it. The CNN consists of 40 kernels (filters) of size 30. Each filter is applied to the input data, performing the convolution. Then, it moves between data by the stride value and performs convolution on the subsequent data, continuing this process until the last data point. Then, by adding bias to the sum of results, the desired filter feature value is obtained. If an activation function exists in the CNN, it is applied at the end. In our network, there is no activation function, and the stride value is one. Additionally, since our CNN has 40 filters, it

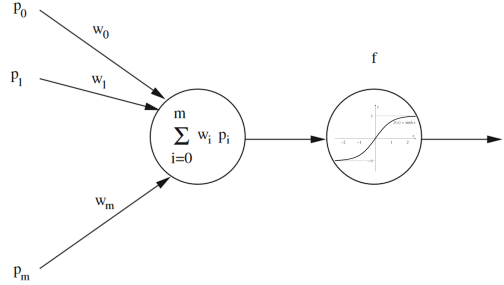


Fig. 6. An overview of the functioning of the DNN network.

will produce 40 outputs. We use “same type padding” in our network, meaning that if the output size of a filter does not match its input, zeros are added equally to both sides to ensure the input and output sizes are the same. Formulas (9) and (10) present the equations related to the CNN and padding [62]–[65]:

$$n_k^l = b_k^l + \sum_{i=1}^{N_{l-1}} \text{conv1D}(w_{ik}^{l-1}, s_i^{l-1}), \quad (9)$$

$$P = \left\lceil \frac{F - 1}{2} \right\rceil, \quad (10)$$

where  $n_k^l$  represents the  $k$ -th neuron in the  $l$ -th layer, and  $b_k^l$  is the bias of the  $k$ -th neuron in the same layer. The operation  $\text{conv1D}$  performs a one-dimensional convolution on the weights  $w_{ik}^{l-1}$  and the features  $s_i^{l-1}$  of the neurons connected to  $n_k^l$ . Here,  $w_{ik}^{l-1}$  refers to the weights connecting neurons from the previous layer to the  $k$ -th neuron,  $s_i^{l-1}$  represents the features and information of the  $i$ -th neuron in the previous layer, and  $N_{l-1}$  denotes the number of neurons in the previous layer. Similarly, in (10),  $P$  denotes the desired padding,  $\lceil \cdot \rceil$  is the operator that rounds the expression up to the nearest integer, and  $F$  represents the size of the convolution filter. After the convolutional network, we have a fully connected layer whose relationships resemble the DNN without an activation function.

We now briefly examine the relationships of the Stochastic Gradient Descent with Momentum (SGDM) optimization algorithm. SGDM is an advanced optimization technique that enhances the basic SGD algorithm by incorporating Momentum. The Momentum component accelerates convergence and smoothens updates, which is especially beneficial in scenarios with high variance or significant oscillations. SGDM achieves this by combining a fraction of the previous gradient update with the current gradient, controlled by a Momentum coefficient (typically close to 1, e.g. 0.9). This approach increases the learning speed and reduces the risk of getting stuck in local minima or saddle points. As a result, SGDM often leads to faster and more stable convergence, making it a popular choice for training deep neural networks in complex, high-dimensional optimization problems [65]–[67]. Model parameters are adjusted via SGDM according to the following relationships:

$$v_t = \rho v_{t-1} + (1 - \rho) \nabla f(x_{t-1}), \quad (11)$$

$$x_t = x_{t-1} - \alpha v_t, \quad (12)$$

where  $\nabla f(x_{t-1})$  represents the gradient of  $f(x_{t-1})$ ,  $v_t$  is the velocity vector at iteration  $t$ ,  $\rho$  is the momentum coefficient,  $x_t$  denotes the model parameters at iteration  $t$ , and  $\alpha$  is the learning rate.

## V. RESULTS AND DISCUSSION

### A. Experimental Setup

To ensure realistic conditions, this experiment is conducted in a two-story building in an urban area with double-layered walls and robust construction materials. The building is significantly distant from BSs, making it an ideal test environment to evaluate our localization algorithm under challenging conditions. Fig. 7 shows the approximate locations of the BSs relative to the building.

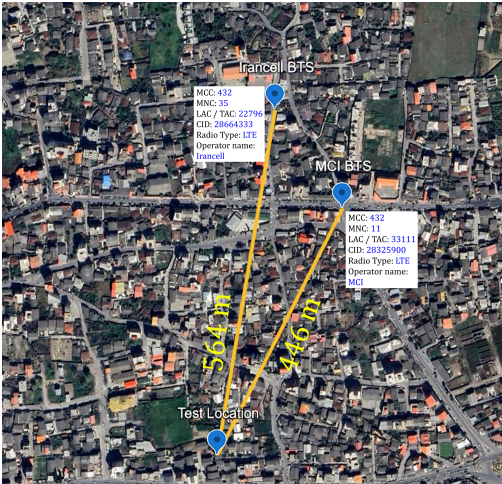


Fig. 7. Approximate locations of the BSs in an urban area.

For measurements, we select a portion of the building's area on both floors. This area, measuring 2.8 by 4 meters, is divided into 34 reference points, 40 centimeters apart. We place the holder base and mobile phone at each reference point. We measure the RSSI parameters of MCI BS with PCI = 301, MTN-Irancell BS with PCI = 161, and the signals of two APs using the software mentioned in Section III. At each point, the RSSI parameters are recorded every second for several minutes, along with the corresponding location and the height of the holder, in a database. This process is repeated on both floors. Each floor has an AP equipped with two 5 dBi antennas operating at a frequency band of 2.4 GHz with a bandwidth of 20 MHz on wireless channel 11. The holder could be adjusted to 68 cm and 108 cm, representing seated and standing positions. We adjust the holder's height to detect user postures and repeat the measurements at the reference points. Thus, our fingerprint database includes user floors, postures, location coordinates, and RSSI parameters. In the database, we label user postures and floors and store the location coordinates in centimeters based on actual measurements. To ensure precise coordinates, we designate one point in the test area as the origin, drew the  $x$  and  $y$  axes from this

point, and then measured each reference point relative to the origin to obtain the location coordinates. Fig. 8 shows the test area and reference points.

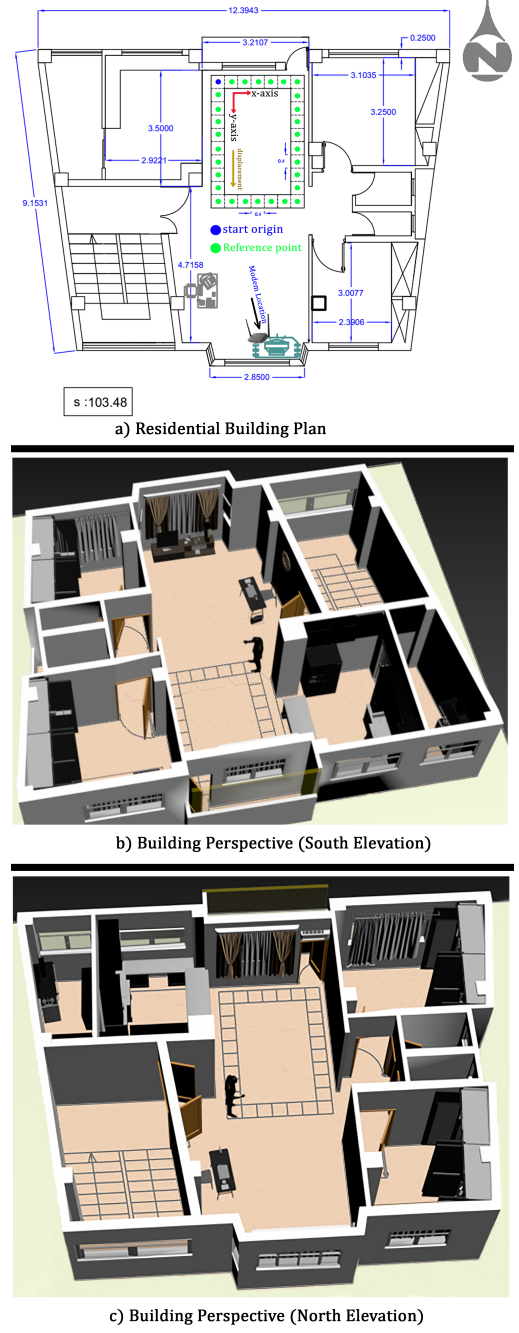


Fig. 8. Layout of the building and reference points.

Now we go for training the neural network. Given that the stored data suffers from severe regression issues and the network cannot learn them well, we modified the fingerprint database to combine data from every three seconds into one row. Each three-second interval corresponds to three RSSI parameters. Thus, the first row contains three parameters from the AP on the first floor, three from the AP on the second floor, three from MCI, and three from MTN-Irancell, summing to 12 parameters. The new database comprises 3,517 rows of

data, with approximately 10% (352 rows) randomly selected as test data and 3,165 rows as training data. As previously explained, the input to our neural network ranges from 6 to 12 neurons, depending on the scenario. The neural network was trained with a learning rate of  $10^{-4}$ , 60,000 epochs, the SGDM optimization algorithm, and a mini-batch size of 16 on a GPU. To detect user postures and floors, we trained separate networks. In other words, we have three neural networks: one for 2D localization and two others for estimating user postures and floor numbers. Fig. 9 provides an overview of the indoor localization process. Additionally, Table I illustrates the settings of the hybrid neural network.

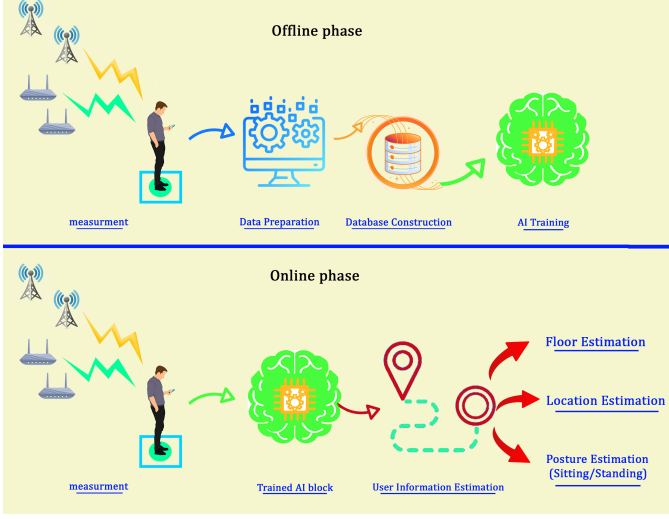


Fig. 9. Overview of the indoor localization process.

TABLE I  
DESIGNED NEURAL NETWORK SETTINGS

Input size	12	DNN activation function	tanh
Output size	2	Optimization Algorithm	sgdm
numEpochs	60000	MiniBatchSize	16
learningRate	0.0001	GradientThreshold	1
convolution Layer (filter size, numFilters)	30,40	Execution Environment	GPU
Number of layers of CNN	1	Number of test samples	352
Deep Neural Network (neuron size)	950	Number of train samples	3165
Number of layers of DNN	4	The total number of database instances	3517
<b>Characteristics of different neural networks tested</b>			
LSTM	LSTM layer (numHiddenUnits)	300	
DNN	Deep Neural Network (neuron size)	950	
	Number of layers of DNN	4	
	DNN activation function	tanh	
1D-CNN	convolution Layer (filter size,numFilters)	30,40	
	Number of layers of CNN	1	
KNN	K, Number Neighbors	3	

### B. Evaluation of Results and Performance Analysis

Table II presents the results across all 4 tested scenarios. This table demonstrates that the implemented model exhibits high accuracy, reliability, and speed, making it highly effective for indoor localization in buildings and commercial spaces. Intuitively, the best result is expected from the 2 BS + 2 AP scenario which can also be seen in the table, nevertheless, all scenarios provide fairly accurate results. In particular, The RMSE and average DE for all scenarios is in the order of 1 meter. Moreover, all 4 cases accurately estimate the floor and the first scenarios is even quite successful in estimating the user posture. From the CDF graphs of 4 scenarios in Fig. 10, we can observe the distribution of distance error which allows us to visualize the proportion of errors that fall below a certain threshold, providing a clear metric to assess accuracy and reliability. For example, a CDF value of 0.90 at 2 meters indicates that 90% of localization errors are within a 2-meter range, demonstrating the effectiveness of our algorithm in achieving precise indoor positioning.

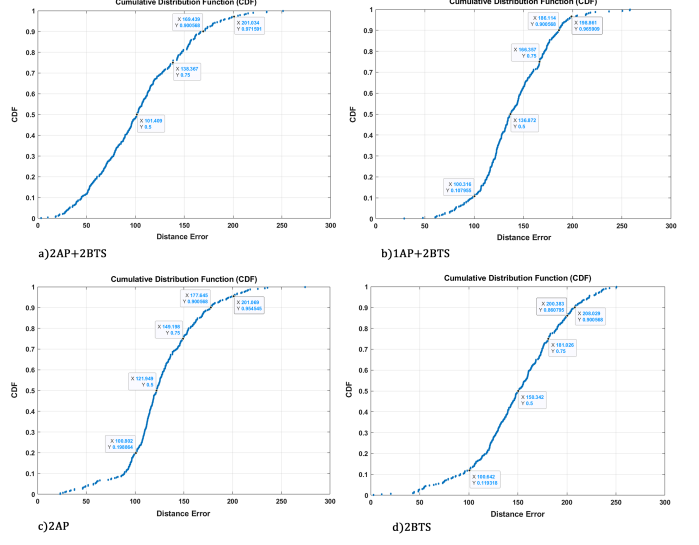


Fig. 10. CDF plots for the four scenarios.

Based on Fig. 11 and Fig. 12, which show the confusion matrices for four different scenarios, we can assess the accuracy of our hybrid model in identifying building floors and user statuses. These matrices indicate that our model can correctly recognize labels in most cases, achieving a high average accuracy across various scenarios. For instance, the model's accuracy in identifying the correct floor labels is over 98% on average, and for user status, it is over 67%. These results indicate the model's capability to accurately identify and categorize data, demonstrating its reliable performance in practical applications.

### C. Examining the Designed Neural Network Model

In this section of the article, we analyze and compare the results of our research with other algorithms and other researchers' work, demonstrating our approach's superiority and efficiency. Table III through Table VI provide a comprehensive

TABLE II  
COMBINED NEURAL NETWORK RESULTS IN ALL SCENARIOS

Scenario Type	2 APs + 2 BSs	1 AP + 2 BSs	2APs	2BSs
Average testing time for each sample	1054.54 $\mu$ s	16522 $\mu$ s	844.88 $\mu$ s	912.5 $\mu$ s
Maximum distance error	251.19 cm	258.3 cm	250.57 cm	274.34 cm
Minimum distance error	3.395 cm	29 cm	2.866 cm	23.21 cm
Average distance error	104.618 cm	140.357 cm	150 cm	126.56 cm
Total RMSE	114.708 cm	144.77 cm	156.77 cm	132.36 cm
RMSE x	62.063 cm	102.468 cm	102.2 cm	94.256 cm
RMSE y	96.468 cm	102.268 cm	118.87 cm	92.921 cm
CDF (50%)	101.4 cm	136.37 cm	150.34 cm	121.95 cm
CDF (75%)	138.37 cm	166.36 cm	181.03 cm	149.2 cm
CDF(90%)	169.44 cm	186.11 cm	208.03 cm	177.64 cm
Floor estimate	accuracy= 99.72%	accuracy= 99.17%	accuracy= 98.58%	accuracy= 99.43%
Estimation of the user's posture (standing/sitting)	accuracy= 88.06%	accuracy= 76.71%	accuracy= 68.75%	accuracy= 67.61%

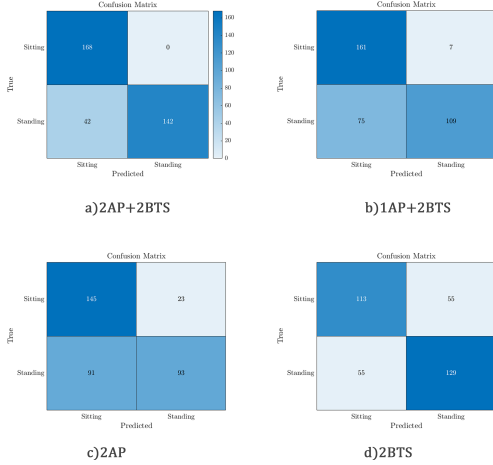


Fig. 11. Confusion matrix for posture recognition.

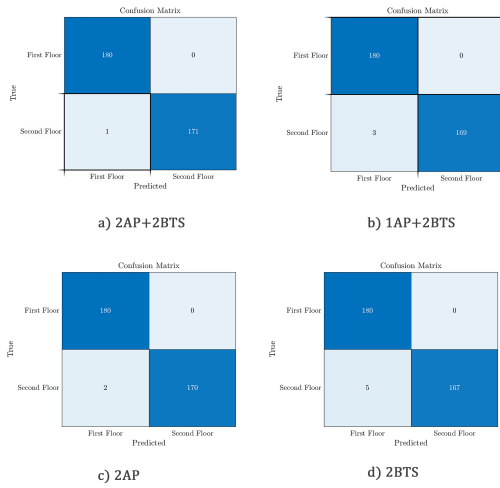


Fig. 12. Confusion matrix for floor recognition.

comparison between our hybrid model and other neural net-

works, such as DNN, LSTM, and CNN, and algorithms, like KNN, decision tree, and SVM, across various scenarios. We can examine all metrics from these tables, including RMSE, CDF, and distance error. This detailed comparison highlights the advantages of our hybrid model in terms of accuracy, robustness, and overall performance in different localization scenarios.

Table III presents the results of various algorithms and AI models in the 2 AP+2 BS scenario. According to this table, the SVM and KNN algorithms outperform the other four algorithms for most parameters, including RMSE, CDF, and user state estimation. Additionally, due to their more straightforward implementation and structure, they have a shorter response time than the other algorithms. However, our hybrid model, due to its complexity and the number of parameters involved, needs more time to respond compared to the different models discussed in this article. Nevertheless, the response time of our model in this scenario is approximately one millisecond, which can be considered satisfactory. Furthermore, our model's RMSE values are between 12% and 20% better, and the CDF values are 9% to 15% better than those of KNN and SVM.

Table IV presents the results for the 1 AP+ 2 BS scenario. Let's focus on the SVM algorithm for comparison as SVM outperforms other algorithms. The SVM algorithm has a shorter response time and a lower average distance error than our model. Additionally, the average distance error in SVM is about 5% better than in our designed model. However, our hybrid model outperforms SVM by 12% in terms of RMSE and by 35% to 40% in CDF at 75th and 90th percentile. Moreover, our hybrid model also maintains superiority in detecting user states and floors.

Table V presents the results for the 2 AP scenario. As shown in Table IV, our hybrid model generally outperforms the other algorithms. Our hybrid model has about 10% lower RMSE, 6% to 15% better CDF values, and approximately 10% lower average distance error compared to the CNN network.

TABLE III  
COMPARISON OF ALGORITHMS IN THE 2 APs + 2 BSs SCENARIO

Algorithm Type	LSTM	CNN	DNN	TREE	SVM	KNN	Our work
Average testing time for each sample	914.77 $\mu$ s	675.56 $\mu$ s	861.36 $\mu$ s	77.55 $\mu$ s	104.83 $\mu$ s	143.75 $\mu$ s	1054.54 $\mu$ s
Maximum distance error	238.35 cm	271.27 cm	228.85 cm	438.321 cm	373.85 cm	422.670 cm	251.19 cm
Minimum distance error	49.9 cm	19.81 cm	124 cm	0 cm	1.57 cm	0 cm	3.395 cm
Average distance error	178.15 cm	137.19 cm	180.06 cm	105.7 cm	105.17 cm	84.767 cm	104.618 cm
Total RMSE	181 cm	144.97 cm	182.74 cm	158.26 cm	131.15 cm	143.38 cm	114.708 cm
RMSE x	107.37 cm	90.46 cm	107.98 cm	104.91 cm	83.84 cm	90.41 cm	62.063 cm
RMSE y	145.73 cm	113.28 cm	147.42 cm	118.5 cm	100.84 cm	111.28 cm	96.468 cm
CDF (50%)	184.4 cm	136.92 cm	187.811 cm	75 cm	82.6 cm	0 cm	101.4 cm
CDF (75%)	204.32 cm	173.3 cm	202.96 cm	195 cm	152.9 cm	164.5 cm	138.37 cm
CDF(90%)	216.45 cm	197.73 cm	216.73 cm	277.31 cm	218.74 cm	269.26 cm	169.44 cm
Floor estimate	accuracy= 100%	accuracy= 96.59%	accuracy= 100%	accuracy= 100%	accuracy= 51.14%	accuracy= 100%	accuracy= 99.72%
Estimation of the user's posture (standing/sitting)	accuracy= 55.4%	accuracy= 55.96%	accuracy= 72.16%	accuracy= 80.11%	accuracy= 83%	accuracy= 84.94%	accuracy= 88.06%

TABLE IV  
COMPARISON OF ALGORITHMS IN THE 1 AP + 2 BSs SCENARIO

Algorithm Type	LSTM	CNN	DNN	TREE	SVM	KNN	Our work
Average testing time for each sample	746.87 $\mu$ s	670.45 $\mu$ s	1056 $\mu$ s	81.53 $\mu$ s	96.3 $\mu$ s	110.22 $\mu$ s	16522 $\mu$ s
Maximum distance error	238.05 cm	275.95 cm	228.85 cm	438.321 cm	371.04 cm	453.48 cm	258.3 cm
Minimum distance error	57.26 cm	11.8 cm	124 cm	0 cm	6.7 cm	0 cm	29 cm
Average distance error	176.96 cm	159.34 cm	180.06 cm	138.8 cm	133.77 cm	136.68 cm	140.357 cm
Total RMSE	179.81 cm	166.85 cm	182.74 cm	193.58 cm	158.84 cm	193.95 cm	144.77 cm
RMSE x	107.52 cm	96.52 cm	107.98 cm	107.18 cm	97.5 cm	116.55 cm	102.468 cm
RMSE y	144.12 cm	136.10 cm	147.42 cm	161.20 cm	125.41 cm	155.01 cm	102.268 cm
CDF (50%)	180.3 cm	165.28 cm	187.822 cm	95.13 cm	120.74 cm	116 cm	136.37 cm
CDF (75%)	199.85 cm	194.87 cm	202.95 cm	253.87 cm	191.43 cm	256 cm	166.36 cm
CDF(90%)	219 cm	216.52 cm	216.74 cm	370 cm	261 cm	346.77 cm	186.11 cm
Floor estimate	accuracy= 99.15%	accuracy= 94.6%	accuracy= 98.86%	accuracy= 99.43%	accuracy= 51.14%	accuracy= 100%	accuracy= 99.17%
Estimation of the user's posture (standing/sitting)	accuracy= 63.92%	accuracy= 58.52%	accuracy= 67.04%	accuracy= 75.56%	accuracy= 75.57%	accuracy= 78.13%	accuracy= 76.71%

Table VI presents the results for the 2 BS scenario, which forms the basis of our study. In this table, the SVM algorithm continues to outperform the other algorithms and is compared with our hybrid model. Our hybrid model outperforms the SVM algorithm by approximately 4% in mean distance error, 15% in RMSE, and 21% to 28% in CDF values.

Table VII is perhaps the most important table in this paper as we compare our with the work of other researchers, examining each study in terms of evaluation criteria, signals, and experimental environments. To do so, we chose 4 excellent works in the literature, [17], [19], [24], [31], that are closer to us in terms of system model. Note that we use two urban BS and two access points for the entire building, which in general much simpler than the first 3 (out of 4 papers) we review here.

In [31], localization was performed separately on each floor to provide two-dimensional localization. The devices used included eight indoor pico BS and specialized measurement

equipment. According to the CDF charts in [31], at 75th CDF percentile, the error is 4 meters on the 2nd floors and 2.5 meters on the 1st floor. In our hybrid model, the 90th CDF percentile is between 1.69 and 2.08 meters.

Chai et al. [24] conducted their research in a corridor of a building using 30 AP devices and six types of BS signals, employing the WKNN algorithm and Manhattan distance. In their best-case scenario, they achieved a maximum distance error of approximately 5.51 meters, a mean distance error of 1.6 meters, and an RMSE of 1.96 meters. In our best-case scenario, our model achieves a maximum distance error of approximately 2.5 meters, a mean distance error of 1.04 meters, and an RMSE of 1.15 meters.

In [17], the researchers investigated indoor localization using the WKNN algorithm. By employing nine small indoor BS and various techniques, they achieved a distance error of approximately 2.7 meters and 90th CDF percentile of 4 meters.

TABLE V  
COMPARISON OF ALGORITHMS IN THE 2 APs SCENARIO

Algorithm Type	LSTM	CNN	DNN	TREE	SVM	KNN	Our work
Average testing time for each sample	650.57 $\mu$ s	720.74 $\mu$ s	864 $\mu$ s	82.38 $\mu$ s	99.72 $\mu$ s	107.95 $\mu$ s	844.88 $\mu$ s
Maximum distance error	235.9 cm	269.6 cm	228.85 cm	452.21 cm	377.86 cm	437.1 cm	250.57 cm
Minimum distance error	51.75 cm	13.9 cm	124 cm	0 cm	5.57 cm	0 cm	2.866 cm
Average distance error	179.93 cm	167.84 cm	180.06 cm	188.76 cm	155.02 cm	201.19 cm	150 cm
Total RMSE	189.79 cm	175 cm	182.74 cm	233.07 cm	177.33 cm	238.82 cm	156.77 cm
RMSE x	107.8 cm	107.5 cm	107.98 cm	129.58 cm	105.15 cm	144.84 cm	102.2 cm
RMSE y	147.62 cm	138.07 cm	147.42 cm	193.73 cm	142.80 cm	189.88 cm	118.87 cm
CDF (50%)	184.54 cm	177.18 cm	187.80 cm	190.4 cm	149.76 cm	240 cm	150.34 cm
CDF (75%)	204.09 cm	200.65 cm	202.95 cm	286.53 cm	220.31 cm	297.07 cm	181.03 cm
CDF(90%)	220.70 cm	222.74 cm	216.73 cm	379.80 cm	273.93 cm	370.54 cm	208.03 cm
Floor estimate	accuracy= 96.59%	accuracy= 54.83%	accuracy= 90.05%	accuracy= 95.45%	accuracy= 49.43%	accuracy= 90.34%	accuracy= 98.58%
Estimation of the user's posture (standing/sitting)	accuracy= 43.75%	accuracy= 55.68%	accuracy= 49.15%	accuracy= 74.15%	accuracy= 74.72%	accuracy= 65.34%	accuracy= 68.75%

TABLE VI  
COMPARISON OF ALGORITHMS IN THE 2 BSs SCENARIO

Algorithm Type	LSTM	CNN	DNN	TREE	SVM	KNN	Our work
Average testing time for each sample	746.02 $\mu$ s	665.34 $\mu$ s	1500 $\mu$ s	82.67 $\mu$ s	81.25 $\mu$ s	108.522 $\mu$ s	912.5 $\mu$ s
Maximum distance error	237.03 cm	283.95 cm	228.85 cm	450.7 cm	400.76 cm	454.86 cm	274.34 cm
Minimum distance error	55.82 cm	56.26 cm	124 cm	0 cm	9.86 cm	0 cm	23.21 cm
Average distance error	177.54 cm	169.3 cm	180.06 cm	150.09 cm	132.45 cm	152.4 cm	126.56 cm
Total RMSE	180.62 cm	173.87 cm	182.74 cm	203.03 cm	155.52 cm	202.15 cm	132.36 cm
RMSE x	105 cm	109.44 cm	107.98 cm	121.96 cm	99.18 cm	124.85 cm	94.256 cm
RMSE y	147 cm	135.11 cm	147.42 cm	162.32 cm	119.8 cm	159 cm	92.921 cm
CDF (50%)	185.4 cm	171.36 cm	187.804 cm	120 cm	122.74 cm	149.16 cm	121.95 cm
CDF (75%)	200.19 cm	196.37 cm	202.96 cm	262.49 cm	190.54 cm	257.1 cm	149.2 cm
CDF(90%)	217.65 cm	219.77 cm	216.73 cm	355 cm	249.6 cm	343.11 cm	177.64 cm
Floor estimate	accuracy= 100%	accuracy= 97.72%	accuracy= 100%	accuracy= 100%	accuracy= 51.14%	accuracy= 100%	accuracy= 99.43%
Estimation of the user's posture (standing/sitting)	accuracy= 42.04%	accuracy= 51.13%	accuracy= 53.12%	accuracy= 65.9%	accuracy= 61.1%	accuracy= 61.36%	accuracy= 67.61%

In our model, with all measurements recorded and evaluated using a simple smartphone, we achieve a maximum distance error of 2.50 meters and 90th CDF percentile of 2.08 meters.

Lee et al. [19] utilized a single PCI in an LTE network to perform indoor localization within a subway station using a correlation technique. Their research was conducted across three scenarios, each representing a different section of the subway station. The resulting RMSE ranges from a minimum of 2.30 meters to a maximum of 2.82 meters. Additionally, the 90th CDF percentile varies from 4.6 meters to 5.1 meters. These results can be compared with those of the 2 BS scenario in our model. In this scenario, our model received signals from two PCI sources, achieving an RMSE of approximately 1.56 meters with 90th CDF percentile of around 2.08 meters. Although Lee's studies utilized only one PCI, which may seem a disadvantage compared to the 2 BS's we utilized, we note that the subway station environment is relatively uniform and

lacks the structural complexities of a residential setting.

## VI. CONCLUSION

Indoor localization using cellular networks is of significant importance as it can fulfill the location need of any special equipment. To enhance the accuracy of localization with this technology, we have taken advantage of accessible technologies and AI methods in this paper: we consider a combination of cellular network with Wi-Fi as an auxiliary network and use a hybrid neural network composed of DNN and CNN networks to improve indoor localization accuracy. In all scenarios, the RMSE on the X and Y axes is estimated to be in order of one meter, providing suitable localization. The deployment of a test system in a two-story residential building with challenging features, confirmed the practical application of our model. The performance of the hybrid network shows considerable improvement in key metrics such

TABLE VII  
COMPARISON OF RESEARCHERS' WORK WITH THIS RESEARCH

Ref.	Algorithm used	Transmitter	Distance Error(DE)	Average DE	RMSE (m)	CDF (m)
[31]	Genetic Algorithm, Neural Network (feedforward-net)	8 (indoor pico BS)	—	—	—	At 75% CDF, the error is more than 4 m on 2 floors and more than 2.5 m on one. The entire building has three floors.
[24]	Manhattan-WKNN K=4	30 AP, BS signals (FD-LTE, WCDMA, CDMA, TD-LTE, TD-SCDMA , GSM)	2 scenarios : max a: 39.24 (m) max b: 5.51 (m)	2 scenarios : a) 3.91 (m) b) 1.60 (m)	2 scenarios : a) 1.96 b) 1.96	CDF 90 % : scenario a: It is between 3 and 4 meters. scenario b: It has not been reviewed.
[19]	2D surface correlation	An LTE signal from PCI 469	—	—	3 scenarios : a) 2.82 b) 2.64 c) 2.30	CDF 90% : a) 4.6 b) 4.8 c) 5.1
[17]	WKNN	9 ( small indoor BS)	2.777 (m)	—	—	CDF 90% : It varies, at least above 4 meters
<b>Our work</b>	A combination of DNN and CNN (specifically designed neural network)	2 BS, 2AP (2PCI: 161, 302 ) 2 Mobile Operators MTN Irancell:161 MCI: 301 AP Brand: D-Link 2 antennas, 5 dBi Wireless channel=11	4 scenarios : max: a) 2.51 (m) b) 2.58 (m) c) 2.74 (m) d) 2.50 (m) min: a) 0.03 (m) b) 0.29 (m) c) 0.23 (m) d) 0.028 (m)	4 scenarios : a) 1.04 (m) b) 1.40 (m) c) 1.26 (m) d) 1.50 (m)	4 scenarios : a) 1.15 b) 1.44 c) 1.32 d) 1.56	CDF 90%: 4 scenarios: a) 1.69 b) 1.86 c) 1.77 d) 2.08

as RMSE and CDF compared to conventional AI methods as well as existing works in the literature. This achievement can aid in developing and enhancing various applications such as the Internet of Things, healthcare, and personnel monitoring. Given the favorable results obtained, this method can be utilized in larger projects and various environments, with an expectation of similar accuracy and efficiency.

## REFERENCES

- [1] F. Alsehly, T. Arslan, and Z. Sevak, "Indoor Positioning with Floor Determination in Multi-Story Buildings," in *Proc. 2011 Int. Conf. Indoor Positioning Indoor Navigation (IPIN)*, Guimaraes, Portugal, 2011, pp. 1-7, doi: 10.1109/IPIN.2011.6071945.
- [2] A. Al-Habashna, G. Wainer, and M. Aloqaily, "Machine Learning-Based Indoor Localization and Occupancy Estimation Using 5G Ultra-Dense Networks," *Simul Model Pract Theory*, vol. 118, p. 102543, 2022, doi: <https://doi.org/10.1016/j.simpat.2022.102543>.
- [3] P. S. Farahsari, A. Farahzadi, J. Rezaizadeh, and A. Bagheri, "A Survey on Indoor Positioning Systems for IoT-Based Applications," *IEEE Internet Things J.*, vol. 9, no. 10, pp. 7680–7699, 2022, doi: 10.1109/JIOT.2022.3149048.
- [4] F. Zafaria, A. Gkelias, and K. K. Leung, "A Survey of Indoor Localization Systems and Technologies," *IEEE Communications Surveys & Tutorials*, vol. 21, no. 3, pp. 2568–2599, 2019, doi: 10.1109/COMST.2019.2911558.
- [5] A. A. Mahdi, A. Chalechale, and A. AbdelRaouf, "A Hybrid Indoor Positioning Model for Critical Situations Based on Localization Technologies," *Mobile Information Systems*, vol. 2022, no. 1, p. 8033380, Jan. 2022, doi: <https://doi.org/10.1155/2022/8033380>.
- [6] A. Ramtohul and K. K. Khedo, "Mobile Positioning Techniques and Systems: A Comprehensive Review," *Mobile Information Systems*, vol. 2020, no. 1, p. 3708521, Jan. 2020, doi: <https://doi.org/10.1155/2020/3708521>.
- [7] R. Joseph and S. B. Sasi, "Indoor Positioning Using Wi-Fi Fingerprint," in *Proc. 2018 Int. Conf. Circuits Syst. Digit. Enterprise Technol. (ICCSDET)*, Kottayam, India, 2018, pp. 1-3, doi: 10.1109/ICCSDET.2018.8821184.
- [8] P. E. Numan, H. Park, C. Laoudias, S. Horsmanheimo, and S. Kim, "Smartphone-Based Indoor Localization via Network Learning with Fusion of FTM/RSSI Measurements," *IEEE Networking Letters*, vol. 5, no. 1, pp. 21–25, 2023, doi: 10.1109/LNET.2022.3226462.
- [9] S. Güney, A. Erdoğan, M. Aktaş, and M. Ergün, "Wi-Fi-Based Indoor Positioning System Using Deep Neural Network," in *Proc. 2020 43rd Int. Conf. Telecommun. Signal Process. (TSP)*, Milan, Italy, 2020, pp. 225–228, doi: 10.1109/TSP49548.2020.9163548.
- [10] N. Singh, S. Choe, and R. Punmiya, "Machine Learning Based Indoor Localization Using Wi-Fi RSSI Fingerprints: An Overview," *IEEE Access*, vol. 9, pp. 127150–127174, 2021, doi: 10.1109/ACCESS.2021.3111083.
- [11] C. A. Gómez-Vega, M. Z. Win, and A. Conti, "UWB Localization-of-Things via Soft Information: Network Experimentation in Indoor Environment," in *Proc. 2023 IEEE Int. Conf. Acoust., Speech Signal Process. (ICASSP)*, Rhodes Island, Greece, 2023, pp. 1-5, doi: 10.1109/ICASSP49357.2023.10094631.
- [12] Y.-M. Lu, J.-P. Sheu, and Y.-C. Kuo, "Deep Learning for Ultra-Wideband Indoor Positioning," in *Proc. 2021 IEEE 32nd Annu. Int. Symp. Personal, Indoor and Mobile Radio Commun. (PIMRC)*, Helsinki, Finland, 2021, pp. 1260–1266, doi: 10.1109/PIMRC50174.2021.9569615.
- [13] F. Pittino, M. Driusso, A. D. Torre, and C. Marshall, "Outdoor and Indoor Experiments with Localization Using LTE Signals," in *Proc. 2017 European Navigation Conf. (ENC)*, Lausanne, Switzerland, 2017, pp. 311–321, doi: 10.1109/EURONAV.2017.7954223.
- [14] H. Zhang, Z. Zhang, S. Zhang, S. Xu, and S. Cao, "Fingerprint-Based Localization Using Commercial LTE Signals: A Field-Trial Study," in *Proc. 2019 IEEE 90th Vehicular Technology Conf. (VTC2019-Fall)*, Honolulu, HI, USA, 2019, pp. 1-5, doi: 10.1109/VTCFall.2019.8891257.
- [15] Y. Wang, K. Zhao, and Z. Zheng, "A 3D Indoor Positioning Method of Wireless Network with Single Base Station in Multipath Environment," *Wirel Commun Mob Comput*, vol. 2022, no. 1, p. 3144509, Jan. 2022, doi: <https://doi.org/10.1155/2022/3144509>.
- [16] Y. You and C. Wu, "Indoor Positioning System With Cellular Network Assistance Based on Received Signal Strength Indication of Beacon," *IEEE Access*, vol. 8, pp. 6691–6703, 2020, doi: 10.1109/ACCESS.2019.2963099.
- [17] H. Zheng, X. Zhong, and P. Liu, "RSS-Based Indoor Passive Localization Using Clustering and Filtering in an LTE Network," in *Proc. 2020 IEEE 91st Vehicular Technology Conf. (VTC2020-Spring)*, Antwerp, Belgium, 2020, pp. 1-6, doi: 10.1109/VTC2020-Spring48590.2020.9128821.

- [18] C.-Y. Chen and W.-R. Wu, "Three-Dimensional Positioning for LTE Systems," *IEEE Trans Veh Technol*, vol. 66, no. 4, pp. 3220–3234, 2017, doi: 10.1109/TVT.2016.2593697.
- [19] J. H. Lee, B. Shin, D. Shin, J. Kim, J. Park, and T. Lee, "Precise Indoor Localization: Rapidly-Converging 2D Surface Correlation-Based Fingerprinting Technology Using LTE Signal," *IEEE Access*, vol. 8, pp. 172829–172838, 2020, doi: 10.1109/ACCESS.2020.3024933.
- [20] W. Fang, C. Xie, and B. Ran, "An Accurate and Real-Time Commercial Indoor Localization System in LTE Networks," *IEEE Access*, vol. 9, pp. 21167–21179, 2021, doi: 10.1109/ACCESS.2020.3034654.
- [21] F. U. Khan, A. N. Mian, and M. T. Mushtaq, "Experimental Testbed Evaluation of Cell-Level Indoor Localization Algorithm Using Wi-Fi and LoRa Protocols," *Ad Hoc Networks*, vol. 125, p. 102732, 2022, doi: <https://doi.org/10.1016/j.adhoc.2021.102732>.
- [22] L. Zhang, X. Chu, and M. Zhai, "Machine Learning-Based Integrated Wireless Sensing and Positioning for Cellular Network," *IEEE Trans Instrum Meas*, vol. 72, pp. 1–11, 2023, doi: 10.1109/TIM.2022.3224513.
- [23] A. Ramamurthy, V. Sathya, M. I. Rochman, and M. Ghosh, "ML-Based Classification of Device Environment Using Wi-Fi and Cellular Signal Measurements," *IEEE Access*, vol. 10, pp. 29461–29472, 2022, doi: 10.1109/ACCESS.2022.3158056.
- [24] M. Chai, C. Li, and H. Huang, "A New Indoor Positioning Algorithm of Cellular and Wi-Fi Networks," *Journal of Navigation*, vol. 73, no. 3, pp. 509–529, 2020, doi: DOI: 10.1017/S0373463319000742.
- [25] Z. Liu, L. Chen, X. Zhou, N. Shen, and R. Chen, "Multipath Tracking with LTE Signals for Accurate TOA Estimation in Indoor Positioning Applications," *Geo-spatial Information Science*, vol. 26, no. 1, pp. 31–43, Jan. 2023, doi: 10.1080/10095020.2022.2108344.
- [26] M. Pan *et al.*, "Efficient Joint DOA and TOA Estimation for Indoor Positioning With 5G Picocell Base Stations," *IEEE Trans Instrum Meas*, vol. 71, pp. 1–19, 2022, doi: 10.1109/TIM.2022.3191705.
- [27] F. Alhomayani and M. H. Mahoor, "Deep Learning Methods for Fingerprint-Based Indoor Positioning: A Review," *Journal of Location Based Services*, vol. 14, no. 3, pp. 129–200, Jul. 2020, doi: 10.1080/17489725.2020.1817582.
- [28] M. Nabati and S. A. Ghorashi, "A Real-Time Fingerprint-Based Indoor Positioning System Using Deep Learning and Preceding States," *Expert Syst Appl*, vol. 213, p. 118889, 2023, doi: <https://doi.org/10.1016/j.eswa.2022.118889>.
- [29] Z. Zhang, M. Lee, and S. Choi, "Deep Learning-Based Indoor Positioning System Using Multiple Fingerprints," in *Proc. 2020 Int. Conf. Inf. Commun. Technol. Convergence (ICTC)*, Jeju, Korea (South), 2020, pp. 491–493, doi: 10.1109/ICTC49870.2020.9289579.
- [30] L. Chen, P. Wen, D. Zou, F. Li, and L. He, "An Innovative Accuracy Estimation Algorithm for Fingerprint Positioning," in *Proc. 2022 Int. Wireless Commun. Mobile Comput. Conf. (IWCMC)*, Dubrovnik, Croatia, 2022, pp. 201–204, doi: 10.1109/IWCMC55113.2022.9825144.
- [31] S. Lembo, S. Horsmanheimo, and P. Honkamaa, "Indoor Positioning Based on RSS Fingerprinting in an LTE Network: Method Based on Genetic Algorithms," in *Proc. 2019 IEEE Int. Conf. Commun. Workshops (ICC Workshops)*, Shanghai, China, 2019, pp. 1–6, doi: 10.1109/ICCW.2019.8756883.
- [32] Y. Ruan *et al.*, "IPos-5G: Indoor Positioning via Commercial 5G NR CSI," *IEEE Internet Things J*, vol. 10, no. 10, pp. 8718–8733, 2023, doi: 10.1109/JIOT.2022.3232221.
- [33] Q. Li, X. Liao, M. Liu, and S. Valaee, "Indoor Localization Based on CSI Fingerprint by Siamese Convolution Neural Network," *IEEE Trans Veh Technol*, vol. 70, no. 11, pp. 12168–12173, 2021, doi: 10.1109/TVT.2021.3107936.
- [34] J. Kaur *et al.*, "AI-Enabled CSI Fingerprinting for Indoor Localization Towards Context-Aware Networking in 6G," in *Proc. 2023 IEEE Wireless Commun. Networking Conf. (WCNC)*, Glasgow, United Kingdom, 2023, pp. 1–5, doi: 10.1109/WCNC55385.2023.10118652.
- [35] X. Ding and S. Dong, "Improving Positioning Algorithm Based on RSSI," *Wirel Pers Commun*, vol. 110, no. 4, pp. 1947–1961, 2020, doi: 10.1007/s11277-019-06821-0.
- [36] T. Zhou, J. Ku, B. Lian, and Y. Zhang, "Indoor Positioning Algorithm Based on an Improved Convolutional Neural Network," *Neural Comput Appl*, vol. 34, no. 9, pp. 6787–6798, 2022, doi: 10.1007/s00521-021-06112-5.
- [37] S. M. Asaad and H. S. Maghdid, "A Comprehensive Review of Indoor/Outdoor Localization Solutions in the IoT Era: Research Challenges and Future Perspectives," *Computer Networks*, vol. 212, p. 109041, 2022, doi: <https://doi.org/10.1016/j.comnet.2022.109041>.
- [38] B. Zhou *et al.*, "DeepVIP: Deep Learning-Based Vehicle Indoor Positioning Using Smartphones," *IEEE Trans Veh Technol*, vol. 71, no. 12, pp. 13299–13309, 2022, doi: 10.1109/TVT.2022.3199507.
- [39] S. Bazin and K. Navaie, "Improving Indoor Positioning Accuracy Using RIS-based RSS Optimization," in *Proc. 2023 Joint Eur. Conf. Networks Commun. & 6G Summit (EuCNC/6G Summit)*, Gothenburg, Sweden, 2023, pp. 663–668, doi: 10.1109/EuCNC/6GSummit58263.2023.10188251.
- [40] S. Sadowski and P. Spachos, "RSSI-Based Indoor Localization With the Internet of Things," *IEEE Access*, vol. 6, pp. 30149–30161, 2018, doi: 10.1109/ACCESS.2018.2843325.
- [41] J. Yan, Z. Huang, and X. Wu, "Smartphone-Based Indoor Localization Using Machine Learning and Multisource Information Fusion," *IEEE Trans Aerosp Electron Syst*, vol. 60, no. 3, pp. 2722–2734, 2024, doi: 10.1109/TAES.2023.3328571.
- [42] C.-H. Hsieh, J.-Y. Chen, and B.-H. Nien, "Deep Learning-Based Indoor Localization Using Received Signal Strength and Channel State Information," *IEEE Access*, vol. 7, pp. 33256–33267, 2019, doi: 10.1109/ACCESS.2019.2903487.
- [43] S. Barai, D. Biswas, and B. Sau, "Distance Measurement Estimation Using NodeMCU ESP8266 Based on RSSI Technique," in *Proc. 2017 IEEE Conf. Antenna Meas. Appl. (CAMA)*, Tsukuba, Japan, 2017, pp. 170–173, doi: 10.1109/CAMA.2017.8273392.
- [44] F. Shang, W. Su, Q. Wang, H. Gao, and Q. Fu, "A Location Estimation Algorithm Based on RSSI Vector Similarity Degree," *Int J Distrib Sens Netw*, vol. 10, no. 8, p. 371350, Aug. 2014, doi: 10.1155/2014/371350.
- [45] Y. Assayag, H. Oliveira, E. Souto, R. Barreto, and R. Pazzi, "Adaptive Path Loss Model for BLE Indoor Positioning System," *IEEE Internet Things J*, vol. 10, no. 14, pp. 12898–12907, 2023, doi: 10.1109/JIOT.2023.3253660.
- [46] H. Huan, K. Wang, Y. Xie, and L. Zhou, "Indoor Location Fingerprinting Algorithm Based on Path Loss Parameter Estimation and Bayesian Inference," *IEEE Sens J*, vol. 23, no. 3, pp. 2507–2521, 2023, doi: 10.1109/JSEN.2022.3227539.
- [47] B. Lee, D. Ham, J. Choi, S.-C. Kim, and Y.-H. Kim, "Genetic Algorithm for Path Loss Model Selection in Signal Strength-Based Indoor Localization," *IEEE Sens J*, vol. 21, no. 21, pp. 24285–24296, 2021, doi: 10.1109/JSEN.2021.3110971.
- [48] Phu Nguyen and David Zwart, "[https://github.com/iamphu/RSSI\\_Logger.git](https://github.com/iamphu/RSSI_Logger.git)," github.
- [49] B. Sulaiman, E. Natsheh, and S. Tarapiah, "Towards a Better Indoor Positioning System: A Location Estimation Process Using Artificial Neural Networks Based on a Semi-Interpolated Database," *Pervasive Mob Comput*, vol. 81, p. 101548, 2022, doi: <https://doi.org/10.1016/j.pmcj.2022.101548>.
- [50] W.-L. Chin, C.-C. Hsieh, D. Shiung, and T. Jiang, "Intelligent Indoor Positioning Based on Artificial Neural Networks," *IEEE Netw*, vol. 34, no. 6, pp. 164–170, 2020, doi: 10.1109/MNET.011.2000096.
- [51] S. F. Ahmed *et al.*, "Deep Learning Modeling Techniques: Current Progress, Applications, Advantages, and Challenges," *Artif Intell Rev*, vol. 56, no. 11, pp. 13521–13617, 2023, doi: 10.1007/s10462-023-10466-8.
- [52] K. Prasanna, "A CNN-LSTM Model for Intrusion Detection System from High Dimensional Data," *Journal of Information and Computational Science*, vol. 10, no. 3, May 2023, doi: 10.5281/zenodo.7911821.
- [53] S. Zhang, X. Li, M. Zong, X. Zhu, and D. Cheng, "Learning K for KNN Classification," *ACM Trans. Intell. Syst. Technol.*, vol. 8, no. 3, Jan. 2017, doi: 10.1145/2990508.
- [54] J. Salvador-Meneses, Z. Ruiz-Chavez, and J. Garcia-Rodriguez, "Compressed KNN: K-Nearest Neighbors with Data Compression," *Entropy*, vol. 21, no. 3, 2019, doi: 10.3390/e21030234.
- [55] P. E. Numan, H. Park, C. Laoudias, S. Horsmanheimo, and S. Kim, "Smartphone-Based Indoor Localization via Network Learning With Fusion of FTM/RSSI Measurements," *IEEE Networking Letters*, vol. 5, no. 1, pp. 21–25, 2023, doi: 10.1109/LNET.2022.3226462.
- [56] Y. You and C. Wu, "Indoor Positioning System With Cellular Network Assistance Based on Received Signal Strength Indication of Beacon," *IEEE Access*, vol. 8, pp. 6691–6703, 2020, doi: 10.1109/ACCESS.2019.2963099.
- [57] M. Cui *et al.*, "A Novel Iterative Positioning Method Based on Difference RSS Model With 5G Field Experiments," *IEEE Sens J*, vol. 24, no. 5, pp. 5466–5475, 2024, doi: 10.1109/JSEN.2023.3277510.
- [58] T. Muškatirović-Zekić, N. Nešković, and D. Budimir, "Efficient Neural Network DPD Architecture for Hybrid Beamforming mMIMO," *Electronics (Basel)*, vol. 12, no. 3, 2023, doi: 10.3390/electronics12030597.
- [59] S. S. Chai, W. L. Cheah, K. L. Goh, Y. H. R. Chang, K. Y. Sim, and K. O. Chin, "A Multilayer Perceptron Neural Network Model to Classify Hypertension in Adolescents Using Anthropometric Measurements: A Cross-Sectional Study in Sarawak, Malaysia," *Comput Math Methods Med*, vol. 2021, no. 1, p. 2794888, Jan. 2021, doi: <https://doi.org/10.1155/2021/2794888>.

- [60] S. BelMannoubi and H. Touati, "Deep Neural Networks for Indoor Localization Using Wi-Fi Fingerprints," in *Mobile, Secure, and Programmable Networking*, É. Renault, S. Boumerdassi, C. Leghris, and S. Bouzefrane, Eds., Cham: Springer International Publishing, 2019, pp. 247–258.
- [61] F. Murtagh, "Multilayer Perceptrons for Classification and Regression," *Neurocomputing*, vol. 2, no. 5, pp. 183–197, 1991, doi: [https://doi.org/10.1016/0925-2312\(91\)90023-5](https://doi.org/10.1016/0925-2312(91)90023-5).
- [62] S. Kiranyaz, T. Ince, O. Abdeljaber, O. Avci, and M. Gabbouj, "1-D Convolutional Neural Networks for Signal Processing Applications," in *Proc. ICASSP 2019 - 2019 IEEE Int. Conf. Acoust., Speech Signal Process.*, Brighton, UK, 2019, pp. 8360–8364, doi: 10.1109/ICASSP2019.8682194.
- [63] Z. Li, F. Liu, W. Yang, S. Peng, and J. Zhou, "A Survey of Convolutional Neural Networks: Analysis, Applications, and Prospects," *IEEE Trans Neural Netw Learn Syst*, vol. 33, no. 12, pp. 6999–7019, 2022, doi: 10.1109/TNNLS.2021.3084827.
- [64] J. Teuwen and N. Moriakov, "Chapter 20 - Convolutional Neural Networks," in *Handbook of Medical Image Computing and Computer Assisted Intervention*, S. K. Zhou, D. Rueckert, and G. Fichtinger, Eds., Academic Press, 2020, pp. 481–501. doi: <https://doi.org/10.1016/B978-0-12-816176-0-00025-9>.
- [65] E. M. Dogo, O. J. Afolabi, N. I. Nwulu, B. Twala, and C. O. Aigbavboa, "A Comparative Analysis of Gradient Descent-Based Optimization Algorithms on Convolutional Neural Networks," in *Proc. 2018 Int. Conf. Comput. Tech., Electron. Mech. Syst. (CTEMS)*, Belgaum, India, 2018, pp. 92–99, doi: 10.1109/CTEMS.2018.8769211.
- [66] Y. Liu, Y. Gao, and W. Yin, "An Improved Analysis of Stochastic Gradient Descent with Momentum," *Adv Neural Inf Process Syst*, vol. 33, pp. 18261–18271, 2020.
- [67] H. Yong, J. Huang, X. Hua, and L. Zhang, "Gradient Centralization: A New Optimization Technique for Deep Neural Networks," in *Proc. Computer Vision-ECCV 2020: 16th Eur. Conf.*, Glasgow, UK, Aug. 23–28, 2020, Proceedings, Part I, Springer, 2020, pp. 635–652.